

S&G 3725

A high frequency magnetotelluric survey of Mount Ruapehu

M.R. Ingham¹ and H.M. Bibby²

¹School of Chemical & Physical Sciences, Victoria University of Wellington, PO Box 600,
Wellington

²GNS Science, PO Box 30368, Lower Hutt



Report prepared for EQC under contract 06/519.

May 2007

Technical Abstract

High frequency magnetotelluric soundings were made at 10 sites on the summit plateau of Mount Ruapehu to investigate the structure and extent of the volcanic hydrothermal system. Three-dimensional inversion of the data shows that beneath the plateau the electrical resistivity is generally low (1-10 Ωm), but that two areas of higher resistivity (~30-100 Ωm) exist. One of these lies at shallow (150-500 m) depth beneath the southern part of the plateau, while the other occurs in a depth range of 1000-1500 m beneath the northern part of the plateau. The extensive low resistivity at shallow depth is interpreted as indicating that the entire summit plateau area has been in contact with volcano/geothermal condensate. The higher resistivity regions are inferred to indicate a change within the hydrothermal system from conductive smectite to resistive chlorite alteration products. This change is temperature controlled, suggesting that the higher resistivity regions are zones of elevated temperature (>150 °C). The difference in depth of the two features would thus imply that a larger thermal gradient exists beneath the southern part of the plateau than the northern area. This is consistent with the existence of a near surface layer of ice which covers the northern part of the plateau, but not the southern. Both resistive regions have very limited lateral extent and are interpreted as being either old volcanic feeders or heat pipes which remain active but have no surface manifestation associated with them.

Laymans Abstract

We have made a series of magnetotelluric measurements on the summit plateau of Mount Ruapehu which allow us to determine the electrical properties of the underlying rocks. In volcanic environments, because of the presence of high temperatures and hydrothermal fluids within the volcanic system, it is expected that the structure will generally be highly electrically conductive. In particular, hydrothermal fluids may cause alteration of the local volcanic rocks to yield products which are more electrically conductive than the original rock. Studies, both elsewhere in the world and within New Zealand geothermal systems, suggest that the nature of these alteration products, and how conductive they are, depends upon the temperature at which they are formed. The products of high temperature alteration are more resistive than those formed at lower temperature.

A 3-dimensional model of the electrical structure of Mount Ruapehu, which explains our observational data, shows that there is indeed widespread low electrical resistivity (high conductivity) beneath the summit plateau and that the structure becomes somewhat less conductive with increasing depth. We believe that this low resistivity is probably caused by steam interacting with shallow groundwater to give extensive acidic alteration. Within this general framework two regions of significantly higher resistivity occur. The first of these is at shallow depth (~150 m) beneath the southern part of the summit plateau and the other at a depth of ~1 km beneath the northern part of the plateau. Tests show that these features are not artefacts of the modelling procedure but are required to provide a good fit to the data. We interpret these regions of lower electrical conductivity to represent areas surrounding heat pipes (or volcanic feeders) where the temperature is high enough that more resistive alteration products have been formed. The general low resistivity environment and the distance of the measurement sites from Crater Lake mean that our data are not sensitive to the similar heat pipe that is assumed to feed the lake. It is clear from the extensive hydrothermal alteration detected across the summit, however, that a much more extensive volcano/hydrothermal system exists (or has existed in the past) beneath the summit of Mount Ruapehu.

We infer that there are two possibilities regarding the heat pipe system we have detected. The first is that the two heat pipes beneath the summit plateau are relict features from past volcanism and are no longer active. This is possibly supported by the fact that the northern resistive feature lies at a greater depth. This may indicate that the rate of increase of temperature with depth is lower beneath the northern part of the summit plateau and that the active volcanic feeder system beneath Mount Ruapehu has moved southwards with time. Alternatively, the two heat pipes beneath the summit plateau may remain active, but have no surface features associated with them.

Introduction

Present knowledge of the hydrothermal/vent system on Mount Ruapehu was derived initially from analysis of the mass and energy budget of Crater Lake (Hurst et al., 1991) and from geochemical analyses (Christenson & Wood, 1993; Christenson, 1994). More recent analyses of the geochemistry (Christenson, 2000) and seismicity (Sherburn et al., 1999; Bryan & Sherburn, 1999), associated with the eruptions of 1995-1996, have supported the earlier inferences of an essentially open vent system allowing significant heat transfer to Crater Lake through a heat pipe. In the upper region of the vent a hydrothermal system which has both single-phase liquid and vapour regions and a two-phase liquid-vapour region is inferred. However no geophysical measurements have been made which can verify the extent of the inferred geothermal/magmatic system.

The aim of this project was to produce an image of the hydrothermal and volcanic vent system on Mount Ruapehu by making high frequency magnetotelluric (MT) measurements on and around the summit plateau. In the MT technique simultaneous measurements of variations in the naturally occurring magnetic and electric fields at the surface of the earth are used to derive the electrical resistivity structure beneath a measurement site. The background electrical resistivity of the earth is generally of the order of 100's - 1000's of Ωm , but within volcanic and geothermal systems factors such as high temperatures, the presence of high salinity fluids, the presence of hydrothermal alteration products and, potentially, magma, all lead to significantly lower resistivity ($\sim 1\text{-}30 \Omega\text{m}$). These systems therefore provide ideal targets for study using geophysical techniques that are sensitive to electrical resistivity. Over the last 10 years MT has become the most widely used technique in the study of volcanic and geothermal systems. Not only have many such systems been studied using MT (e.g. Aizawa et al., 2005; Manzella et al., 2004; Matsushima et al., 2001; Monteiro Santos et al., 2006; Muller & Haak, 2004; Nurhasan et al., 2006; Takakura & Matsushima, 2003), but it has also proved possible to relate resistivity variations to the detailed structure of hydrothermal systems.

The project has formed the basis for an MSc Thesis "High frequency magnetotelluric survey of the volcanic vent and hydrothermal system on Mount Ruapehu, New Zealand" by Keleigh Anne Jones (Jones, 2007). Full details of the theory, measurements, data analysis and modelling are given in the thesis.

Magnetotelluric Sounding

In a magnetotelluric sounding temporal variations in the horizontal components of the naturally occurring electric field at the surface of the Earth are measured through the use of perpendicular electric dipoles of length ~ 50 m which use non-polarising electrodes for contact with the ground surface. Variations in the horizontal magnetic field components are measured using appropriately oriented induction coil magnetometers. In this project data were recorded using three Phoenix Geophysics Limited MTU-5A 24 bit data acquisition units belonging to GNS Science.

At an individual frequency the components of the electric (\underline{E}) and magnetic (\underline{B}) fields are related through the impedance tensor \underline{Z}

$$\underline{E} = \underline{Z}\underline{H} \quad (1)$$

where $\underline{B} = \mu_0 \underline{H}$, μ_0 being the permeability of free-space. More explicitly, in terms of components of the fields

$$\begin{aligned} E_x &= Z_{xx}H_x + Z_{xy}H_y \\ E_y &= Z_{yx}H_x + Z_{yy}H_y \end{aligned} \quad (2)$$

in which the four impedance tensor elements contain information on the electrical resistivity structure beneath the measurement site. The penetration depth of the MT method depends upon the frequency of the variations in the magnetic and electric fields that are being measured. The skin depth, a measure of the penetration, is given by

$$\delta = \sqrt{\frac{2\rho}{\mu_0\omega}} \quad (3)$$

where ρ is the ambient electrical resistivity and ω is the angular frequency of the variation. It can be seen from (3) that lower frequency variations contain information on deeper structure. Consequently measurements over a range of frequencies can provide information over a sufficient range of depth scales that a complete picture of the variation of resistivity with depth may be derived.

The variation of the impedance tensor with frequency is usually presented in terms of plots of apparent resistivity and phase against the period (T) of the variation. For an impedance tensor element Z_{ij} , apparent resistivity (ρ_a) and phase (ϕ_a) are defined by

$$\rho_a = \frac{1}{\mu_0\omega} |Z_{ij}|^2 \quad (4)$$

$$\phi_a = \tan^{-1} \frac{\text{Im}(Z_{ij})}{\text{Re}(Z_{ij})} \quad (5)$$

The resistivity structure associated with a given set of measurements is derived by matching the calculated impedances due to a model structure to the measured apparent resistivity and phase curves from the available data sites.

Measurements and data analysis

MT measurements were made at a total of 10 sites on the summit plateau of Mount Ruapehu (Fig. 1). Following an earlier attempt, aborted due to bad weather, measurements at 9 of these sites were made over the period of 30-31 March 2006. The other site (site 117) was measured during a previous MT study of the deeper electrical structure of the Mount Ruapehu region (Dravitzki, 2005). The original intention was to obtain measurements from up to 15 sites, including at sites adjacent to Crater Lake. However, even at minimum snow cover in late March, measurements to the south of the Dome shelter were infeasible due to the steep topography and residual snow/ice cover combining to make access to the area immediately north of the lake impossible. Measurements on the then existing tephra dam on the south side of the lake would have been possible, but deteriorating weather conditions prevented extension of the measurement period.

Latitude, longitude, altitude, recording times and the basic frequency range of the data for the measured sites are listed in Table 1. For the depth range of interest in this study (a few kilometres) it was estimated that the longest period data necessary was of the order of 1 s. To achieve this a recording time of the order of 2-3 hours was estimated to be sufficient to obtain enough quality data in the frequency range 300- 1 Hz. Consequently, data at sites 601, 602, 606, 607 and 608 were recorded for just under 3 hours. Even with this relatively short recording time at these sites, estimates of the impedance tensor \underline{Z} were obtained down to a frequency of

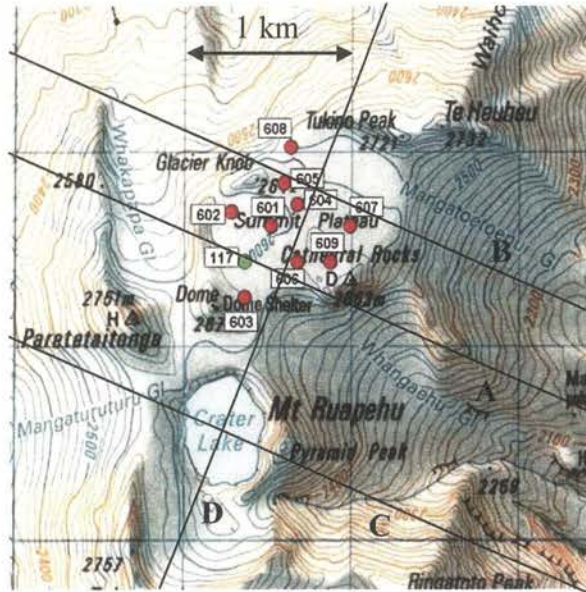


Figure 1: Locations of MT sites on the summit plateau of Mount Ruapehu. Lines A, B, C and D refer to the sections through the final resistivity model discussed below.

Site	Site Location			Recording time (h)	Nominal frequency range (Hz)
	Long. (°)	Lat. (°)	Altitude (m)		
601	175.5672	-39.2716	2606	2.6986	320-0.001
602	175.5645	-39.2708	2581	2.9647	320-0.001
603	175.5657	-39.2749	2598	20.2994	320-0.0005
604	175.5690	-39.2704	2609	20.5081	320-0.0005
605	175.5679	-39.2696	2610	20.7467	320-0.0005
606	175.5692	-39.2730	2606	2.8219	320-0.001
607	175.5728	-39.2713	2595	2.9492	320-0.001
608	175.5684	-39.2679	2587	2.1236	320-0.001
609	175.5715	-39.2728	2614	0.9014	320-0.004
117	175.5655	-39.2732	2592	21.8311	320-0.0005

Table 1: Site locations, recording times and frequency ranges.

approximately 0.001 Hz. At sites 603, 604, 605 and 117, where the equipment was left to record overnight, high quality impedance estimates were obtained down to a frequency of 0.0005 Hz. Measurements at site 609 on 31 March had to be curtailed due to rapidly deteriorating weather conditions. As a result, although the nominal frequency range of data at site 609 is from 320-0.001 Hz, the useable frequency range over which estimates of the impedance tensor had small uncertainties is significantly shorter. Following the completed measurements it was discovered that one electrode dipole at sites 601, 604 and 607 had suffered from an intermittent poor connection. At sites 601 and 607, with shorter recording times, only one electric field orientation could subsequently be used. At site 604 where data were recorded overnight it proved possible to recover the complete impedance tensor.

601



602

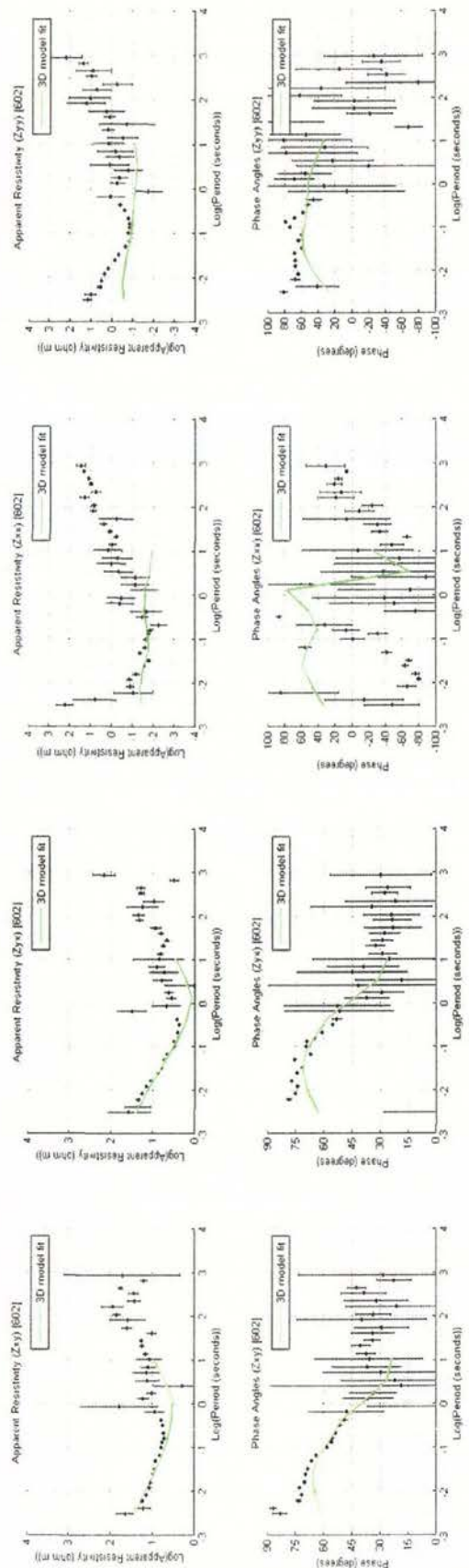
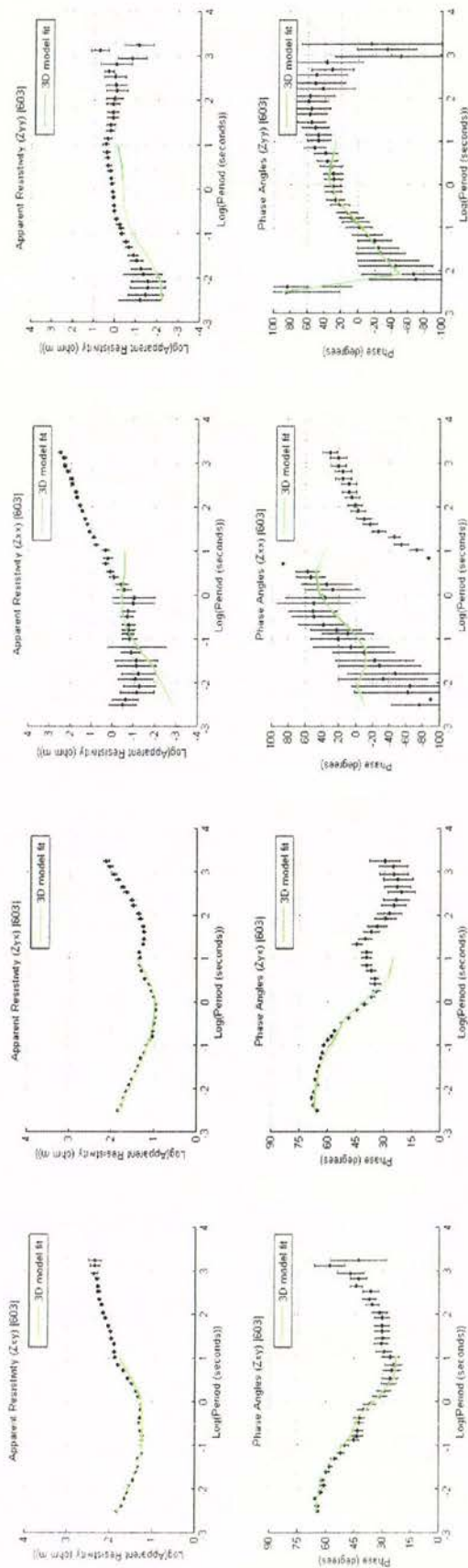


Figure 2(a): Measured apparent resistivity and phase data for site 601, apparent resistivity and phase data after distortion correction for site 602. Green lines show the calculated response of the 3-dimensional resistivity model.

603



604

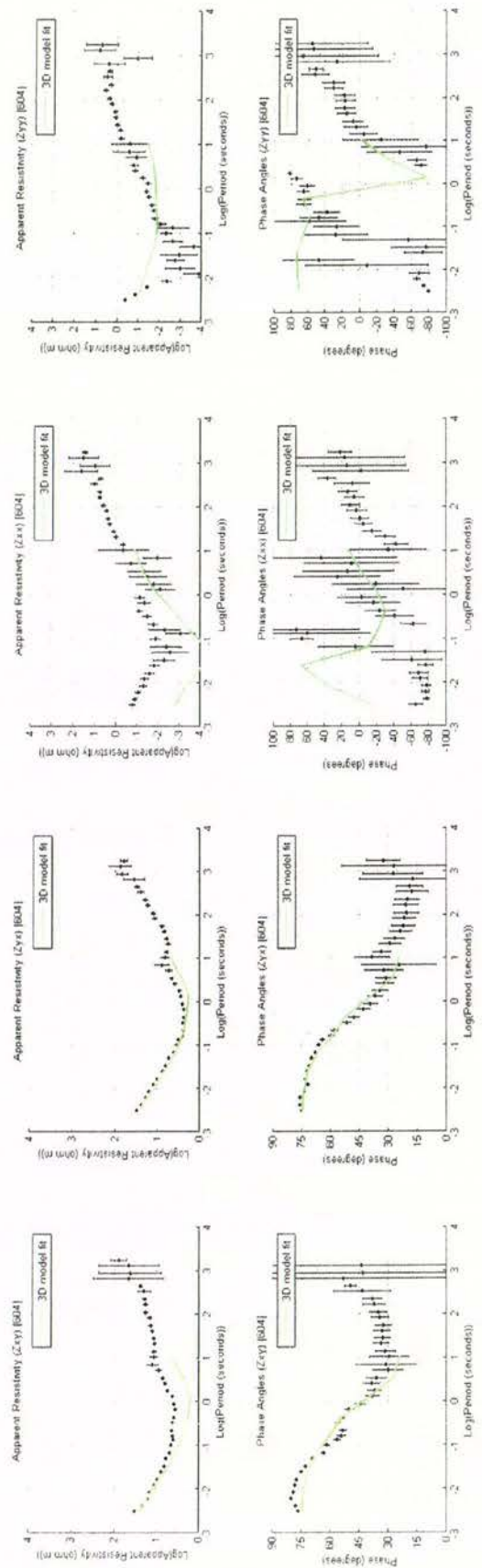
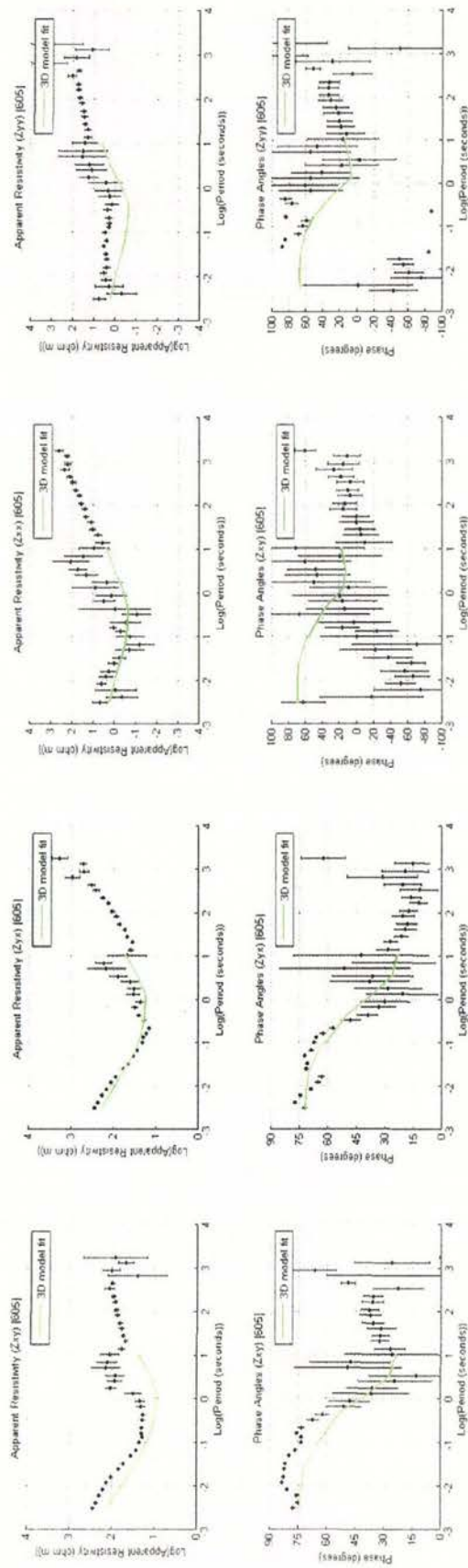


Figure 2(b): Apparent resistivity and phase data after distortion correction for sites 603 and 604. Green lines show the calculated response of the 3-dimensional resistivity model.

605



606

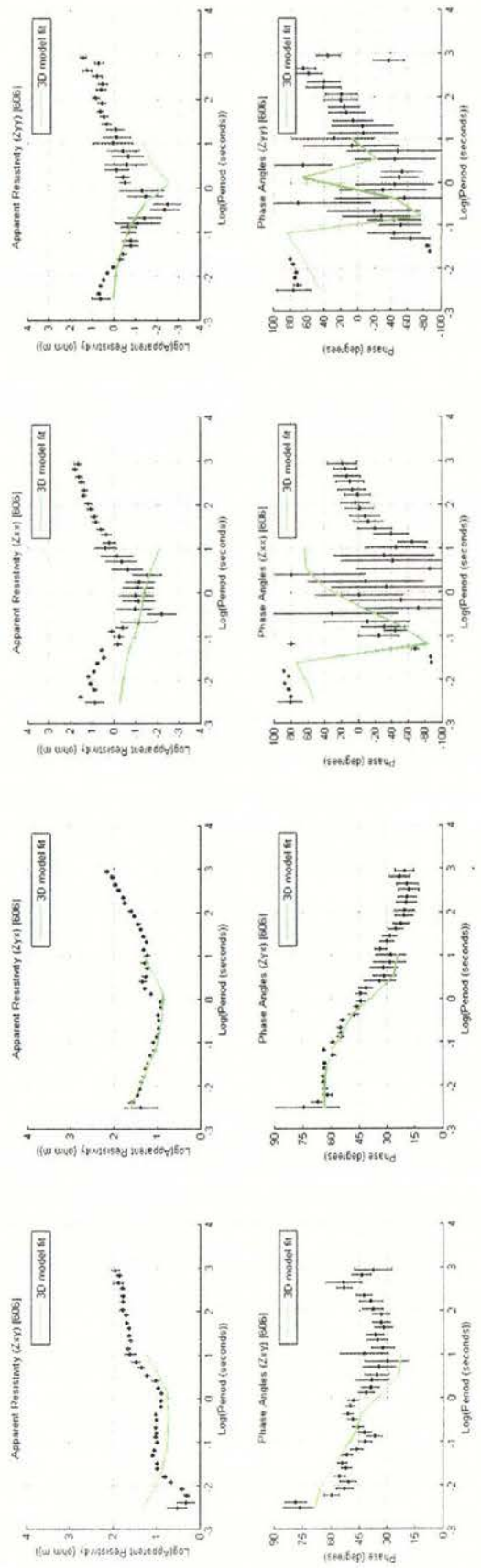


Figure 2(c): Apparent resistivity and phase data after distortion correction for sites 605 and 606. Green lines show the calculated response of the 3-dimensional resistivity model.

607



608

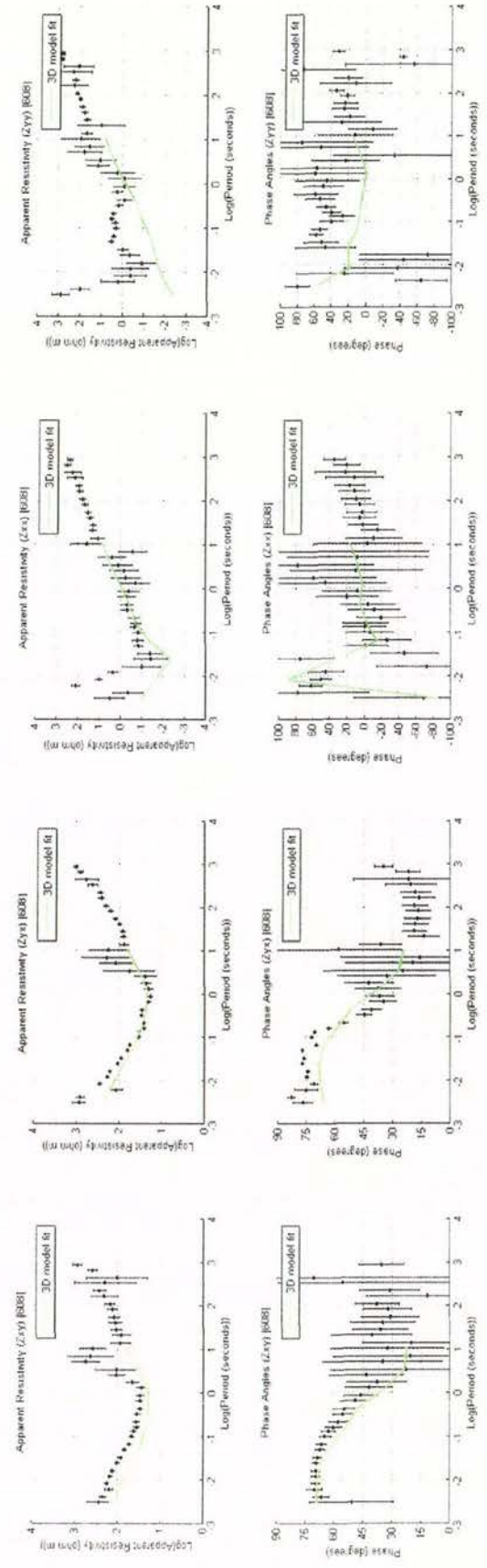
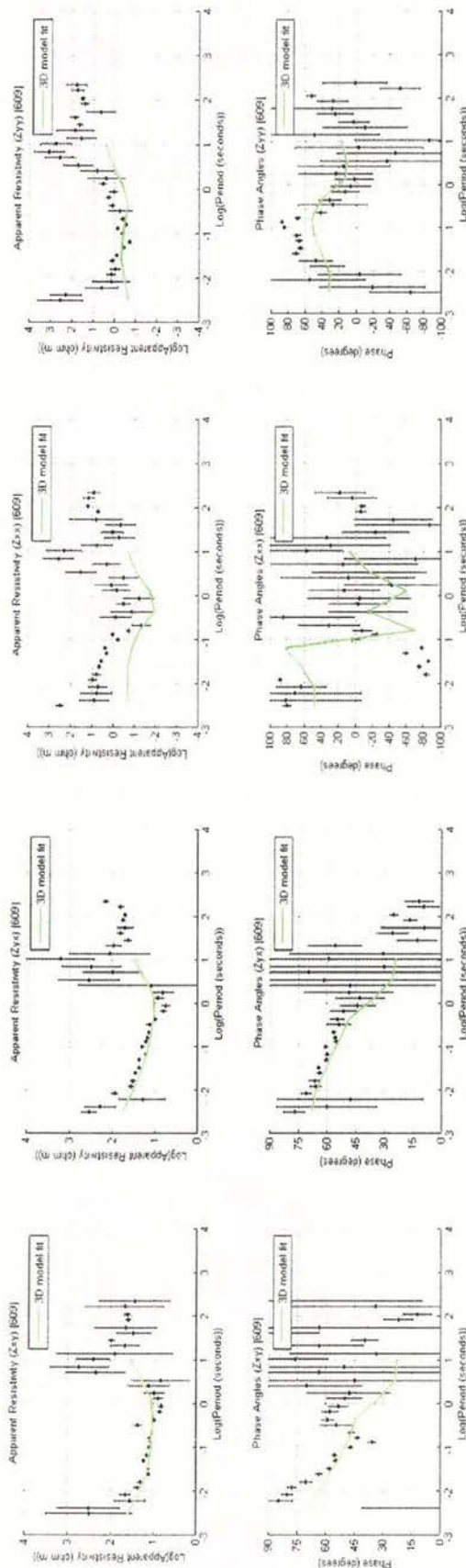


Figure 2(d): Measured apparent resistivity and phase data for site 607, apparent resistivity and phase data after distortion correction for site 608. Green lines show the calculated response of the 3-dimensional resistivity model.

609



117

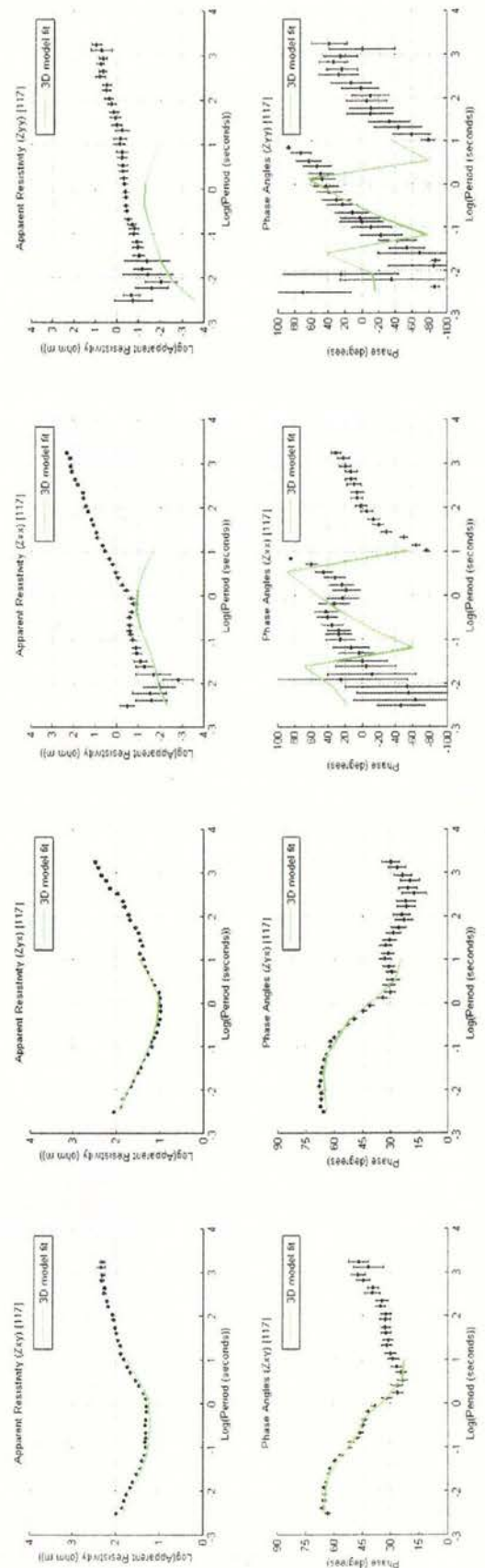


Figure 2(e): Measured apparent resistivity and phase data for site 609, apparent resistivity and phase data after distortion correction for site 117. Green lines show the calculated response of the 3-dimensional resistivity model.

Post-processing of the recorded data (using the robust processing program SSMT2000 (Version 2.5, March 2005) produced by Phoenix Geophysics Limited) to obtain initial estimates of the impedance tensor as a function of variation frequency was followed by distortion analysis using the phase tensor technique of Caldwell et al. (2004) and Bibby et al. (2005). This analysis yields information on the dimensionality of the electrical resistivity structure and also, as long as some portion of the recorded frequency range can be identified as being responsive to 1-dimensional structure (i.e. a variation of resistivity with depth only), also allows for the removal of galvanic distortions in the impedance tensor data. Such distortions result from small scale inhomogeneities in structure. Full details of the distortion analysis as carried out on the data is given by Jones (2007). The resulting apparent resistivity and phase curves for sites 602, 603, 604, 605, 606, 608 and 117 after the distortion analysis are shown in Fig. 2. Distortion analysis was not possible for sites 601 and 607 where only one electric field component was recorded, and at sites 602 and 609 no frequency range in which the data were responsive to 1-dimensional structure could be identified. For these sites the curves presented in Fig. 2 are those of the original data. In Fig. 2, and in other figures displaying the results of the inversion, the co-ordinate system relates to magnetic north, thus, for example, the impedance tensor element Z_{xy} relates the electric field variations in the magnetic north direction in response to the magnetic field variations in the magnetic east direction.

It can be seen from the data presented in Fig.2 that smooth curves of apparent resistivity and phase estimates calculated from the principle impedance tensor elements (Z_{xy} and Z_{yx}) have been obtained at all sites in the period range 0.005 - 3 s. Despite some scatter in estimates over the dead band (1 - 10 s period) where the natural signal strength is low, quite good quality data has been obtained out to periods of around 1000 s at all sites except 602 and 609. As expected, although the data are more scattered, the apparent resistivity estimates derived from the diagonal elements of the impedance tensor are significantly smaller at shorter periods than those derived from Z_{xy} and Z_{yx} , suggesting that at shallow depths the resistivity structure is 1-dimensional, i.e. varies only with depth.

Modelling and inversion

A three dimensional model of the resistivity structure beneath the summit plateau was derived using the 3D inversion program WSINV3DMT (Sirirunvaraporn et. al. 2005). An initial, or starting, model for the inversion was created using results of preliminary 1-dimensional modelling as a guide. This initial model consisted of a 150 Ω m surface layer, underlain at 150m depth by a relative conductor with a resistivity of 10 Ω m and a thickness of 1.85 km. Underlying this was a resistivity of 275 Ω m. Topography was included in the inversion by finding the average elevation in each square of the model grid and assuming a resistivity of 10¹² Ω m to represent air. The resistivity of these 'air' cells was fixed during the inversion. The complete model grid covered a lateral area of 100 km² centred on the summit plateau and extended to a depth of 20 km. To provide detailed horizontal resolution, the area of main interest - the summit plateau - was divided into square cells of side length 62.5 m. The data included in the inversion were taken at nine periods spread approximately two per decade over the period range 0.003125s – 10.66667s. This excluded poorly estimated longer period values of the impedance tensor at those sites with shorter recording times.

The derived resistivity structure is shown in the form of four sections (Figs. 1 & 3) through the resulting 3-dimensional model. Sections A and B are oriented magnetic EW and are located south and north of the centre of the summit plateau respectively. Section C is an EW

section through Crater Lake. Section D is a magnetic NS section located just to the east of the centre of the summit plateau. All sections have a total length of 10 km. Horizontal slices through the derived model, covering only the area of the summit plateau are shown in the Appendix. The green curves in Fig. 2 show the degree to which the observed data are fit by the apparent resistivity and phase curves calculated from the derived model structure.

As can be seen from Fig.2 the fit of the derived model to the data is excellent. Small apparent resistivity misfits in Z_{xy} at sites 604 and 608 can probably be attributed to unresolved static shift. Caused by small very localised variations in surface conditions, static shift results in the apparent resistivity curves being offset by a constant factor although the phase remains unchanged. At short period at site 606 the apparent resistivity misfit in Z_{xy} and Z_{yx} is believed to be the result of topographic effects not accounted for in the model structure. The fit of the model to the apparent resistivity and phase data calculated from the off-diagonal elements of the impedance tensor is also good, although the much smaller magnitude of Z_{xx} and Z_{yy} mean that misfits to these elements are much less significant.

The derived structure (Fig. 3) shows that beneath a thin resistive surface layer, the summit plateau of Ruapehu is characterised by generally low electrical resistivity. In the upper 500-1000 m typical resistivity values are in the range 3-10 Ω m. Against this low resistivity background two features of significance stand out. These are two areas, marked R1 and R2 in Fig. 4, have a resistivity an order of magnitude higher than the general background. Region R1, at a depth of between 150 and ~500 m, lies beneath the southern part of the summit plateau. Region R2 has a slightly higher resistivity, at a depth of 1000-1500 m, and lies beneath the north-central part of the plateau. The lateral locations of R1 and R2 are clearly shown in Fig. 4, which shows horizontal slices through the 3-dimensional model at the appropriate depths. To test how well these resistive regions are constrained by the data, each has in turn been removed from the final model which has then been used as the starting model for a new inversion. In both cases the resistive region which had been removed was reinstated by the new inversion with a significant reduction in the rms residual. It can be concluded therefore that both regions R1 and R2 are required to adequately fit the data.

Interpretation

Low resistivity is measured at shallow depths across the entire plateau. Such low resistivities are a typical near surface feature of geothermal systems throughout the Taupo Volcanic Zone and are caused by low temperature hydrothermal alteration of the volcanic rocks which produces conductive clays. The extensive low resistivity suggests that the entire area has been in contact with volcano/geothermal condensate, resulting from the interaction of rising heated volcanic gases with groundwater. Typical bicarbonate rich waters formed by this interaction can be found in seeps on the north-east flanks of Ruapehu.

For most volcanic rocks of the central North Island of New Zealand resistivity decreases with depth (e.g. Bibby et al., 1992). However, it has also been observed that within high temperature geothermal systems resistivity tends to increase with depth (e.g. Bibby et. al., 1992; Risk et. al.; 1999; Björnsson et. al., 1986). Björnsson et. al. (1986) gives a number of possible explanations for higher resistivity to occur at depth within a hydrothermal system. These include the suggestion of a change in alteration minerals with temperature and in turn with depth, from conductive smectite to resistive chlorite. This idea of a change of alteration mineral has recently been used in the interpretation of a study of the hydrothermal system of Kusatsu-Shirane volcano, Japan (Nurhasan et. al. 2006) in which a modelled conductive zone

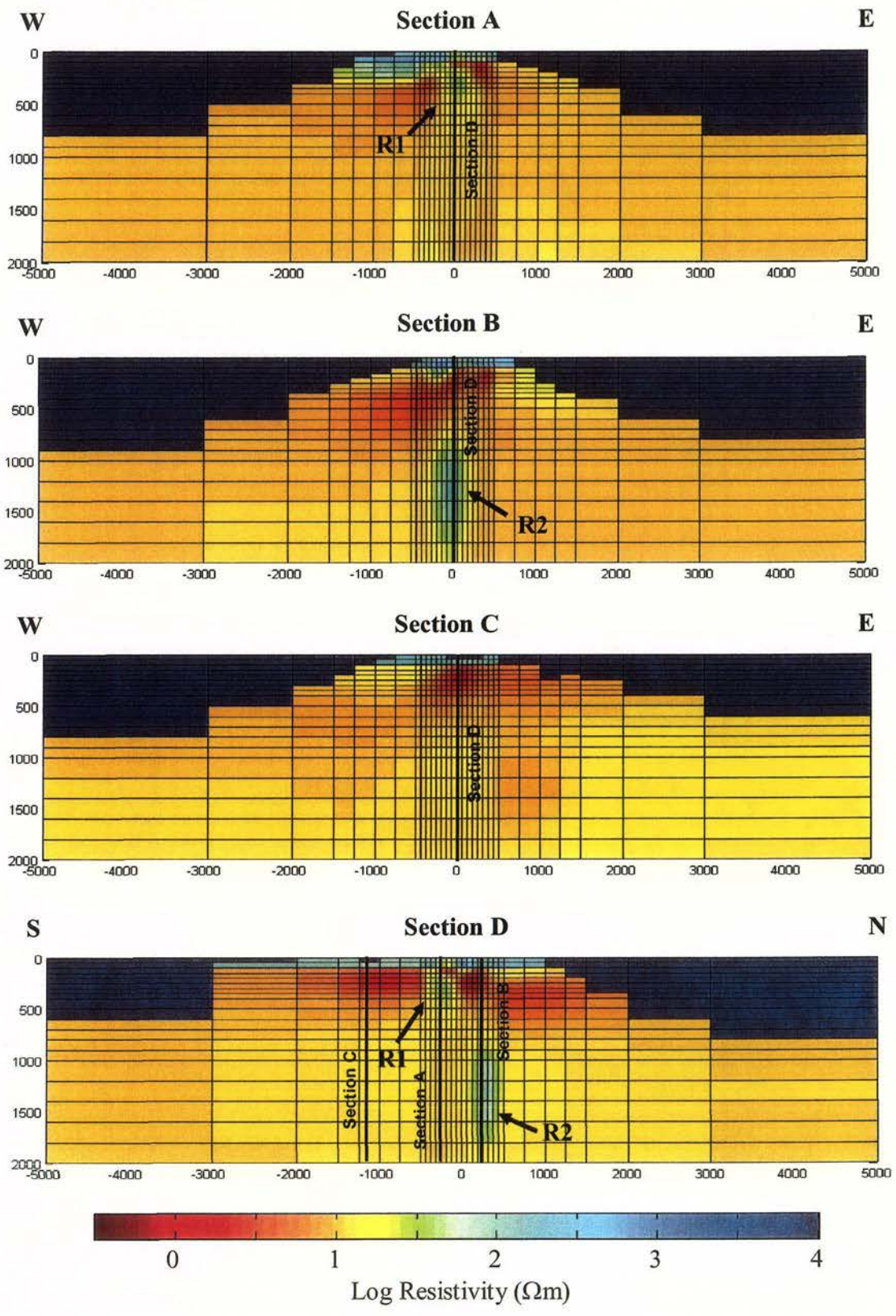


Figure 3: Vertical sections through the derived 3-dimensional resistivity structure.

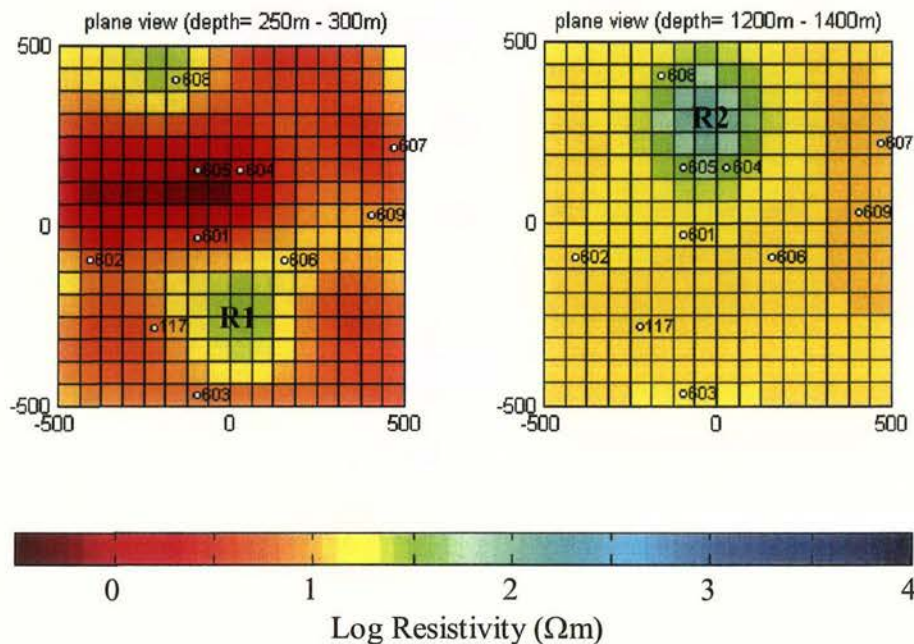


Figure 4: Horizontal slices through the 3-D model showing regions R1 and R2.

overlying a deeper higher resistivity layer is explained by an electrically conductive Montmorillonite clay mineral overlying a zone in which clay minerals are dominated by resistive chlorite and quartz minerals. The two resistive regions (R1 and R2) seen in the 3-dimensional resistivity model for Mount Ruapehu (Figs. 3 and 4) may be explained similarly by a change in alteration product from conductive smectite to resistive chlorite clay.

Such a change in alteration mineral is reliant on increasing temperature. As noted by Bibby et al. (1992) an increase in resistivity, indicative of the change in alteration mineral, will occur in hydrothermal systems where the temperature increases monotonically with depth. Bibby et al. (1992) quote an average temperature of around 150°C for the first appearance of chlorite. For the characteristic temperature-depth profile observed in geothermal systems in New Zealand, chlorite would thus be expected to be first encountered at depths of the order of 100m – 200m. The depth at which the shallower southern resistor (R1) is first seen (~150 m) is consistent with these values. Crater Lake which is the visible focus of hydrothermal activity on Ruapehu is situated approximately 350 m SE (with respect to magnetic north) of site 603 and is roughly 100m lower than the summit plateau. The thermal vents which were visible following the eruption of 1995-96 lie about 40 meters lower than the lake level, at about the same elevation as the top of the shallow resistor beneath the plateau. Although it was not covered by the survey data, it is probable that the low resistivity at shallow depth which lies beneath the summit plateau extends to encompass the Crater Lake area as well.

Within this low resistivity framework the observed greater depth of R2 may indicate a smaller temperature gradient beneath the northern part of the summit plateau, so that resistive alteration products occur at greater depth. Some support for this variation in thermal gradient is suggested by the observation that, at a depth of ~ 1m beneath the surface material, the northern part of the summit plateau is underlain by a layer of ice. Such a layer does not exist beneath the southern part of the plateau. Given the similar surface conditions in both areas it

can be hypothesised that the formation of an ice layer beneath the southern part of the summit plateau is prevented by increased heat flow resulting from a higher temperature gradient.

The two resistive areas of hydrothermal alteration products, which are also laterally constrained, are identified as possible candidates for an extensive heat pipe system such as that suggested by Hurst et. al. (1991). How such a system connects to Crater Lake itself initially appears problematic as the 3-dimensional model (e.g. Fig. 4(d) and (e)) shows no similar feature to exist beneath the lake. This dichotomy is resolved when it is realised that the extensive shallow low resistivity beneath the lake means that data from MT sites on the summit plateau are actually insensitive to deeper structure beneath Crater Lake. This can be demonstrated by inserting a similar higher resistivity region to R1 and R2 into the final model structure beneath the lake, and using this amended model as a starting point for a new inversion. In this case the added resistive feature is not removed by the new inversion indicating that the observational data are not sensitive to structure in this area of the model.

A sketch of the inferred heat pipe system below Mount Ruapehu, in relationship to the observed resistivity structure, is shown in Fig. 5. Given that the present active centre of volcanic activity is Crater Lake, the question remains as to whether features R1 and R2 represent older volcanic feeders and imply that the active centre of Mount Ruapehu volcanism has moved southwards with time, or whether one or both of these features still represents an active heat pipe but without surface manifestation. If a region with high

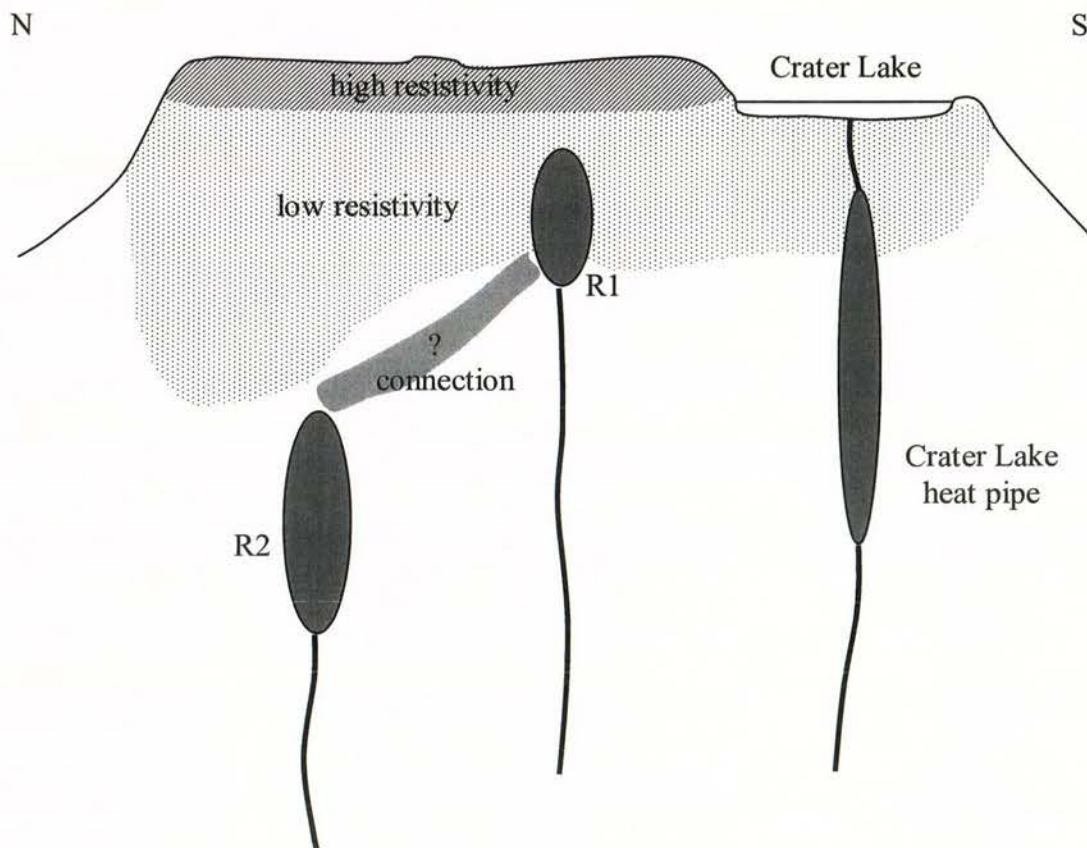


Fig. 5: Sketch of the possible heat pipe system under Mount Ruapehu and its relationship to the modelled resistivity structure.

temperature alteration were to become cooled the continued presence of volcanic gases would in time also change the chemistry of the zone so that the alteration was in equilibrium with its surroundings. This does not rule out the possibility that the observed high temperature zones may have been much larger in the past, but means that some continued hydrothermal activity is required for their maintenance. We suggest therefore that the summit area may have been the site of more active hydrothermal activity in the past, but that current activity has migrated towards Crater Lake which is the current active centre.

Discussion

The initial aim of this project was to identify finite limits of the hydrothermal system beneath the Mount Ruapehu plateau. From the results it is apparent, that rather than being able to identify the boundaries of the hydrothermal system, the entire area of the summit plateau is underlain by hydrothermally altered volcanic rocks, even though no hydrothermal features are visible on the summit. A minimum area of the hydrothermal system would encompass the Crater Lake, giving an area of $\sim 1 \text{ km}^2$. The two areas of higher resistivity beneath the summit plateau are interpreted to be regions enclosing high temperature alteration products, as are observed at depth within the geothermal systems of the TVZ. These narrow features may represent feeder zones for escaping volcanic gasses although we speculate that the summit area may have been the centre of hydrothermal activity in the past. Without any equivalent data from pre-1995 it is not clear how much of the present day signature is related to the eruptions of 1995-96. In particular it is possible that the extensive area of alteration may be due to the massive outpourings of heated gases that occur during periods of eruption, and thus mark the response to periodic episodes rather than being the steady state condition that is the norm. This would imply that the summit hydrothermal system is undergoing a recovery phase, consistent with the narrow high temperature feeder zones observed beneath the plateau. If this is correct it raises the question as to whether monitoring changes in the summit system may provide an alternative way of detecting changes to the hydrothermal system associated with eruption episodes?

References

- Aizawa, K., Yoshimura, R., Oshiman, N., Yamazaki, K., Uto, T., Ogawa, Y., Tank, S. B., Kanda, W., Sakanaka, S., Furukawa, Y., Hashimoto, T., Uyeshima, M., Ogawa, T., Shiozaki, I. & Hurst, A. W., 2005. Hydrothermal system beneath Mt Fuji volcano inferred from magnetotellurics and electric self potential. *Earth Planet. Sci. Lett.*, 235, 343-355
- Bibby, H. M., Dawson, G. B., Rayner, H. H., Bennie, S. L. & Bromley, C. J., 1992. Electrical resistivity and magnetic investigations of the geothermal systems in the Rotorua area, New Zealand. *Geothermics*, 21, 43-69
- Bibby, H. M., Caldwell, T.G. & Brown, C., 2005. Determinable and non-determinable parameters of galvanic distortion in magnetotellurics. *Geophys. J. Int.*, 163, 915-930.
- Björnsson, A., Hersir, G. P. & Björnsson, G., 1986. The Hengill high-temperature area SW-Iceland: Regional geophysical survey. *Geothermal Resources Council Transactions*, 10, 205-210.
- Bryan, C.J. & Sherburn, S., 1999. Seismicity associated with the 1995-1996 eruptions of Ruapehu volcano, New Zealand: a narrative and insights into physical processes. *J. Volcan. Geotherm. Res.*, 90, 1-18.
- Caldwell, T. G., Bibby, H. M. & Brown, C., 2004. The magnetotelluric phase tensor. *Geophys. J. Int.*, 158, 457-469
- Christenson, B.W. & Wood, C.P., 1993. Evolution of a vent-hosted hydrothermal system beneath Ruapehu Crater Lake, New Zealand. *Bull. Volcanol.*, 55, 547-565.
- Christenson, B.W., 1994. Convection and stratification in Ruapehu Crater Lake, New Zealand: implications for Lake Nyos-type gas release eruptions. *Geochem. J.*, 28, 185-198.
- Christenson, B.W., 2000. Geochemistry of fluids associated with the 1995-1996 eruption of Mt. Ruapehu, New Zealand: signatures and processes in the magmatic-hydrothermal system. *J. Volcan. Geotherm. Res.*, 97, 1-30.
- Dravitzki, S. M., 2005. Structural and Hydrothermal Inferences from a Magnetotelluric survey across Mt. Ruapehu, New Zealand. Unpublished MSc Thesis, School of Earth Sciences, Victoria University of Wellington.
- Hurst, A.W., Bibby, H.M., Scott, B.J. & McGuinness, M.J., 1991. The heat source of Ruapehu Crater Lake; deductions from the energy and mass balances. *J. Volcan. Geotherm. Res.*, 46, 1-20.
- Jones, K.A., 2007. High frequency magnetotelluric survey of the volcanic vent and hydrothermal system on Mount Ruapehu, New Zealand. Unpublished MSc Thesis, School of Chemical and Physical Sciences, Victoria University of Wellington.
- Manzella, A., Volpi, G., Zaja, A. & Meju, M., 2004. Combined TEM-MT investigation of shallow-depth resistivity structure of Mt Somma-Vesuvius. *J. Volcan. Geotherm. Res.*, 131, 19-32.

Matsushima, N., Oshima, H., Ogawa, Y., Takakura, S., Satoh, H., Utsugi, M. & Nishida, Y., 2001. Magma prospecting in Usu volcano, Hokkaido, Japan, using magnetotelluric soundings. *J. Volcan. Geotherm. Res.*, 109, 263-277.

Monteiro Santos, F. A., Trota, A., Soares, A., Luzio, R., Lourenco, N., Matos, L., Almedia, E., Gaspar, J. L. & Miranda, J. M., 2006. An audio-magnetotelluric investigation in Terceira Island (Azores). *Journal of Applied Geophysics*, 59, 314-323

Müller, A. & Haak, V., 2004. 3-D modelling of the deep electrical conductivity of Merapi volcano (Central Java): integrating magnetotellurics, induction vectors and the effects of steep topography. *J. Volcan. Geotherm. Res.*, 138, 205-222

Nurhasan, Ogawa, Y., Ujihara, N., Tank, S. B., Honkura, Y., Onizawa, S., Mori, T. & Makino, M., 2006. Two electrical conductors beneath Kusatsu-Shirane volcano, Japan, imaged by audiomagnetotellurics, and their implications for the hydrothermal system. *Earth Planets Space*, 58, 1053-1059

Risk, G. F., Bibby, H. M. & Caldwell, T. G., 1999. Resistivity structure of the central Taupo Volcanic Zone, New Zealand. *J. Volcan. Geotherm. Res.*, 90, 163-181.

Sherburn, S., Bryan, C.J., Hurst, A.W., Latter, J.H. & Scott, B.J., 1999. Seismicity of Ruapehu volcano, New Zealand, 1971-1996: a review. *J. Volcan. Geotherm. Res.*, 88, 255-278.

Siripunvaraporn, W., Egbert, G., Lenbury, Y. & Uyeshima, M., 2005. Three-dimensional magnetotelluric inversion: data-space method. *Phys. Earth Planet. Int.*, 150, 3-14.

Takakura, S. & Matsushima, N., 2003. Magnetotelluric investigation of the hydrothermal system and heat source in the Muine-Toyoha geothermal area, Hokkaido, Japan. *Resource Geology*, 53, 213-220.

Appendix A

Horizontal slices through the final 3-D resistivity model. Depths are below the summit plateau. Horizontal scales are in m.

